

RESEARCH

Open Access



Slow-fast dynamics of Hopfield spruce-budworm model with memory effects

Na Wang^{1,2*} and Maoan Han²

*Correspondence:
wangna1621@126.com
¹Department of Applied
Mathematics, Shanghai Institute of
Technology, Shanghai, 201418,
China

Abstract

In this paper we consider a kind of the spruce-budworm system with memory effects. On the basis of geometric singular perturbation theory, the transition of the solution trajectory is illustrated, and the existence of the relaxation oscillation with a rapid movement process alternating with a slow movement process is proved. The characteristic of the relaxation oscillation, it is indicated, is dependent on the structure of the slow manifold. Moreover, the approximate expression of the relaxation oscillation and its period are obtained analytically. Finally we present two simulations to demonstrate the validity of the analytical conclusion.

MSC: 34M60; 34C26

Keywords: geometric singular perturbation; relaxation oscillations; memory effects

1 Introduction

To reproduce the dynamics of the spruce-budworm system, the Hopfield spruce-budworm model has been proposed in the work of Rasmusse *et al.* [1] who showed for a spruce-budworm model that the predator and prey permanently oscillate for any positive initial conditions. Such kinds of spruce-budworm systems exhibit periodic outbreaks at about 40 year intervals in North-American forests. During outbreaks, populations of the budworm may multiply hundredfold in a few months, causing severe defoliation. Trees are seldom killed by defoliation, and they may live for 100-150 years, but it takes them 7-10 years to fully regrow their leaves.

In [2], Ludwig *et al.* proposed a model separating the timescales of slow spruce regrowth versus the fast population dynamics of budworm larvae and their predators. They used the so-called logistic model for the food-limited dynamics of budworms in the absence of predators. Birds preying on budworms were assumed to exhibit a switching functional response [3], searching for other food resources when the population of budworm is low, and switching to budworm only when the density of budworm exceeds a certain threshold. Following [2, 3] Rasmusse *et al.* study the model

$$\begin{cases} \dot{N}(t^*) = rN(1 - \frac{N}{kS}) - \beta \frac{PN^2}{\eta^2 S^2 + N^2}, \\ \dot{S}(t^*) = \rho S(1 - \frac{S}{S_{\max}}) - \delta N, \end{cases} \quad (1.1)$$

where N and S represent the budworm population density and the spruce biomass density, respectively. By using singular perturbation theory, a relaxation oscillation of this system was obtained.

As pointed out in [4, 5], the existence of such relaxation oscillations implies that the coexistence of predators and prey occurs through a simple periodically alternated two-season behavior: a poor season, characterized by an almost endemic presence of the prey, alternates with a rich season, during which prey are abundant and predators are regenerated.

It is natural to introduce time delay into models of interacting species, formulated in the coupled ordinary differential equation [6–11]. For example, in predator-prey models it is reasonable to assume that the rate of increase of the prey population depends on the recent history of the prey population. So, in this study we propose and analyze the following spruce-budworm system of equations:

$$\begin{cases} \dot{N}(t^*) = rN(t^*)\left(1 - \frac{N(t^*)}{kS(t^*)}\right) - \beta \frac{P(N(t^*))^2}{\eta^2(S(t^*))^2 + (N(t^*))^2}, \\ \dot{S}(t^*) = \rho S(t^*)\left(1 - \frac{\int_{-\infty}^{t^*} W(t^*-z)S(z) dz}{S_{\max}}\right) - \delta N(t^*), \end{cases} \quad (1.2)$$

which describes the dynamics of interactions between a predator and a prey species with a distributed delay $W(t^* - z)$ in the prey population $S(t^*)$, at time t^* . The parameters r , ρ , k , β , P , δ , η , and S_{\max} are positive. r is the intrinsic growth rate for the budworm population, ρ is a typical growth rate for the biomass population, k is the effective carrying capacity coefficient for the budworm, β is the maximum consumption rate of budworms per budworm-predator per time, P is the maximal loss of budworm due to higher order predators, δ is per capita rate for spruce depletion per budworm per time, η is the effective regulation coefficient for the predation pressure, S_{\max} is the 'carrying capacity' (asymptotic maximum) of the leaf area, kS is the carrying capacity for the budworm population, ηS is the half-saturation density of the predator pressure, δN is the predation pressure on the prey (leaves), and $\beta \frac{PN^2}{\eta^2 S^2 + N^2}$ represents the predation pressure by a lose term due to the relatively fast timescale of predation.

The distributed delay represented by the weight function $W(s) : R^+ \rightarrow R^+$ satisfies $W(s) \geq 0$ and $\int_0^\infty W(t^*) dt = 1$. See [12–14]. The continuous delay in the prey equation means that the quantity of prey has an influence on the present growth rate of prey not just at a single moment in the past but over the whole past, or at least in those time intervals where the function $W(t^*)$ is not zero. Our study in this paper treats the case of the density function $W(s) : R^+ \rightarrow R^+$ defined by

$$W(s) = a^2 s e^{-as}, \quad a > 0, \quad (1.3)$$

which is the term called the 'strong' generic kernel function ('memory with hump') and is a particular case of the Gamma function described by Fargue [15]. The 'strong' generic kernel implies that a particular time in the past is more important than any other [16].

If the weight function in model (1.2) is given by (1.3), we have the advantage that it specifies the moment in the past when the quantity of the prey is most important from the point of view of the present growth of the prey. This occurs $\frac{1}{a}$ units before the present time t (the weight function has a hump at $z = t - \frac{1}{a}$, and going further backwards in time the effect of the past is fading away), the phenomenon is richer. And when the delay kernel

function $W(s)$ takes the form of the ‘strong’ generic kernel function, it is unknown how the delay kernel $W(s) = a^2 s e^{-as}$ ($a > 0$) (i.e., the parameter a) affects the dynamics of system (1.2). Therefore, in this paper, we study mainly the effects of the parameter a in the ‘strong’ delay kernel on the dynamical behaviors of system (1.2).

Though our study in this paper allows one to replace the distributed delay $W(s)$ given in (1.2) by a more general Gamma distributed delay kernel, for example

$$W(s) = \frac{a^m s^{m-1} e^{-as}}{(m-1)!}, \quad m = 3, 4, \dots, n, \quad (1.4)$$

we prefer to retain the second equation in system (1.2) in its present form only as the mathematical calculations are very complicated.

The present paper is organized as follows. In Section 2, by means of a change of variables, we first transform system (1.2) with the ‘strong’ delay kernel into a four-dimensional system of differential equations. In Section 3, by linearizing the resulting four-dimensional system at the positive equilibrium and analyzing the associated characteristic equation, the Hopf bifurcations are demonstrated. In particular, by applying geometric singular perturbation theory, the approximate expression of the relaxation oscillation and its period are obtained analytically. To verify our theoretical predictions, two numerical simulations are also included in Section 4.

As argued by Ludwig *et al.* [2], we assume that the predator population in our model has fast dynamics (the predator population grows much faster than those of the predator), i.e., $\rho \ll r$.

2 The model equation

We define two new variables as

$$Q(t^*) = \int_{-\infty}^{t^*} W(t^* - z) S(z) dz = a^2 \int_{-\infty}^{t^*} (t^* - z) S(z) e^{-a(t^* - z)} dz$$

and

$$R(t^*) = a \int_{-\infty}^{t^*} S(z) e^{-a(t^* - z)} dz.$$

Then using the *linear chain trick technique* (see [17]), system (1.2) can be transformed into the following equivalent system:

$$\begin{cases} \dot{N}(t^*) = rN(t^*)\left(1 - \frac{N(t^*)}{kS(t^*)}\right) - \beta \frac{P(N(t^*))^2}{\eta^2(S(t^*))^2 + (N(t^*))^2}, \\ \dot{S}(t^*) = \rho S(t^*)\left(1 - \frac{Q(t^*)}{S_{\max}}\right) - \delta N(t^*), \\ \dot{Q}(t^*) = a(R(t^*) - Q(t^*)), \\ \dot{R}(t^*) = a(S(t^*) - R(t^*)). \end{cases} \quad (2.1)$$

To simplify expression of (2.1), we introduce a new time variable $\tau = \rho t^*$, and denote $\varepsilon = \frac{\rho}{r}$, $X = \frac{N}{kS}$, $Z = \frac{rN}{\beta P}$, $Y = \frac{rkS}{\beta P}$, $Y_{\max} = \frac{rkS_{\max}}{\beta P}$, $\alpha = \frac{\eta}{k}$, $\varrho = \frac{k\delta}{\rho}$, and $V = \frac{rkQ}{\beta P}$, $U = \frac{rkR}{\beta P}$. Then

equation (2.1) is referred to as the *dimensionless spruce-budworm model*,

$$\begin{cases} \varepsilon \frac{dZ}{d\tau} = YF_0\left(\frac{Z}{Y}, Y; \alpha^2\right), \\ \frac{dY}{d\tau} = Yf\left(\frac{Z}{Y}, V; \varrho, Y_{\max}\right), \\ \frac{dV}{d\tau} = f^*(V, U; a), \\ \frac{dU}{d\tau} = g^*(Y, U; a), \end{cases} \quad (2.2)$$

where

$$F_0(X, Y; \alpha^2) = X(1 - X) - \frac{1}{Y} \cdot \frac{X^2}{\alpha^2 + X^2},$$

$$f(X, V; \varrho, Y_{\max}) = 1 - \frac{V}{Y_{\max}} - \varrho X,$$

$$f^*(V, U; a) = a(U - V),$$

$$g^*(Y, U; a) = a(Y - U),$$

and $0 < \varepsilon \ll 1$. The small positive parameter ε in this system implies that model (2.2) is a singularly perturbed system. The possible non-trivial equilibrium points satisfy the conditions

$$Y = \frac{X}{(\alpha^2 + X^2)(1 - X)}, \quad (2.3)$$

$$V = Y_{\max}(1 - \varrho X), \quad (2.4)$$

$$Y = U = V. \quad (2.5)$$

Since $X, Y > 0$, it follows from (2.3)-(2.5) that possible equilibrium points are restricted to the strip $0 < X < 1$ and $Y, V, U > 0$.

We introduce a fast time variable $t = \frac{\tau}{\varepsilon}$, and denote $Z(t) = Z(\varepsilon t)$, $Y(t) = Y(\varepsilon t)$, $V(t) = V(\varepsilon t)$, and $U(t) = U(\varepsilon t)$, then equation (2.2) becomes

$$\begin{cases} \frac{dZ}{dt} = YF_0\left(\frac{Z}{Y}, Y; \alpha^2\right), \\ \frac{dY}{dt} = \varepsilon Yf\left(\frac{Z}{Y}, V; \varrho, Y_{\max}\right), \\ \frac{dV}{dt} = \varepsilon f^*(V, U; a) \\ \frac{dU}{dt} = \varepsilon g^*(Y, U; a). \end{cases} \quad (2.6)$$

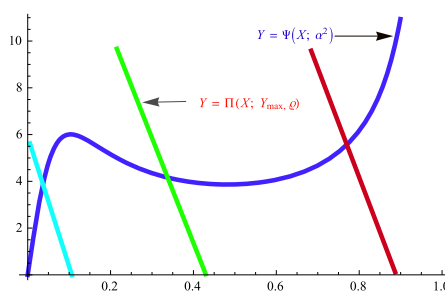
Letting $\varepsilon \rightarrow 0$ in equation (2.6), one has a fast subsystem governing the fast variable only

$$\frac{dZ}{dt} = YF_0\left(\frac{Z}{Y}, Y; \alpha^2\right), \quad (2.7)$$

where Y is regarded as a parameter.

Remark 1 The model with the delay kernel $W(s)$ is very hard to analyze. So authors use many methods to eliminate delay. By defining new variables and using the linear chain trick technique, the original model (1.2) can be rewritten as the equivalent ordinary differential

Figure 1 Three different cases of the one equilibrium point in the strip $0 < X < 1$ and $Y > 0$ when $0 < \alpha^2 = 0.0085 < \frac{1}{27}$ with the projection on the (X, Y) plane.



equations (2.2) without delay. But the price is that the dimension of the equations would be increased from two to four. Although the model becomes the four-dimensional system (2.2), the variables U and V of the systems do not play a major role. Therefore, we only need to analyze the first two equations of (2.2).

3 Slow-fast dynamics

Geometric singular perturbation theory, mainly due to Tikhonov and Fenichel [18–21], is an efficient tool for investigating the slow-fast dynamics of the systems with two timescales. According to the geometric singular perturbation theory, the dynamical behavior of the two timescale systems is governed by the structure of the slow manifold including the shape, stability, and bifurcation of the slow manifold, as well as the location and stability of the equilibrium of the two timescale systems.

First, the geometric singular perturbation theory defines the slow manifold of equation (2.6) as the equilibriums of the fast subsystem equation (2.7)

$$\begin{aligned} M &= \left\{ (Z, Y, V, U) \mid YF_0\left(\frac{Z}{Y}, Y; \alpha^2\right) = 0 \right\} \\ &= \left\{ (Z, Y, V, U) \mid Y = \frac{X}{(\alpha^2 + X^2)(1 - X)} \right\}, \end{aligned} \quad (3.1)$$

where $X = \frac{Z}{Y}$. It is the phase space for the reduced problem. Denote $\Psi(X; \alpha^2) := \frac{X}{(X^2 + \alpha^2)(1 - X)}$, $\Pi(X; Y_{\max}, \varrho) := Y_{\max}(1 - \varrho X)$. From $Y = \frac{X}{(\alpha^2 + X^2)(1 - X)}$, we have

$$\frac{dY}{dX} = \Psi'(X; \alpha^2) = \frac{\mathbb{P}_3(X)}{(X^2 + \alpha^2)^2(1 - X)^2}, \quad (3.2)$$

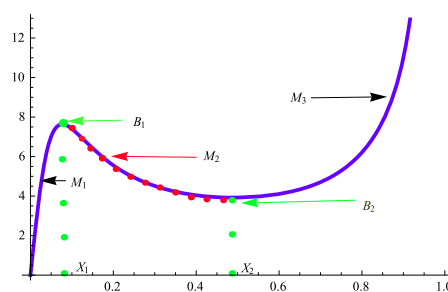
where $\mathbb{P}_3(X) = 2X^3 - X^2 + \alpha^2$.

The shape of the slow manifold depends on the coefficient α^2 . In the following discussion, the case with an S-shape curve of the slow manifold is focused on, correspondingly, we let α^2 satisfy $0 < \alpha^2 < \frac{1}{27}$ (see Figure 1).

To determine the stability and bifurcation of the slow manifold M , let us consider the stability of the equilibriums of the fast subsystem equation (2.7). For any equilibrium point (Y_0, X_0) , the linearized system is

$$\frac{dZ}{dt} = \left[1 - 2X_0 - \frac{2\alpha^2 X_0}{Y_0(\alpha^2 + X_0^2)^2} \right] Z(t). \quad (3.3)$$

Figure 2 The structure of the slow manifold M of equation (2.6) with the projection on the (X, Y) plane, where B_1 and B_2 are the saddle-node bifurcation points.



In the slow manifold M , the one eigenvalue of equation (3.3) is

$$\lambda = 1 - 2X_0 - \frac{2\alpha^2 X_0}{Y_0(\alpha^2 + X_0^2)^2}.$$

As for λ , there are two critical points X_1 and X_2 satisfy with $0 < X_1 < \frac{1}{3} < X_2 \leq \frac{1}{2} < 1$ such that $\lambda > 0$ with $X_0 \in (X_1, X_2)$ and $\lambda < 0$ with $X_0 \in (0, X_1) \cup (X_2, 1)$. The stable branches and the unstable branch meet in bifurcation points which can be shown to represent two saddle-node points [1], denoted by $B_1 = (Z_1, Y_1, V_1, U_1)$ and $B_2 = (Z_2, Y_2, V_2, U_2)$, where $Z_i = X_i Y_i$, $V_i = U_i = Y_i$, $\frac{X_i}{(X_i^2 + \alpha^2)(1 - X_i)} = Y_i$, and $\mathbb{P}_3(X_i) = 0$ ($i = 1, 2$). The slow manifold M is divided into three parts by the bifurcation points B_1 and B_2 ,

$$M = M_1 + M_2 + M_3,$$

here

$$\begin{aligned} M_1 &= \left\{ (Z, Y, V, U) \mid Z = XY, Y = \frac{X}{(X^2 + \alpha^2)(1 - X)}, 0 < X < X_1 \right\}, \\ M_2 &= \left\{ (Z, Y, V, U) \mid Z = XY, Y = \frac{X}{(X^2 + \alpha^2)(1 - X)}, X_1 < X < X_2 \right\}, \\ M_3 &= \left\{ (Z, Y, V, U) \mid Z = XY, Y = \frac{X}{(X^2 + \alpha^2)(1 - X)}, X_2 < X < 1 \right\}, \end{aligned}$$

and M_2 is unstable, M_1 and M_3 are stable, as illustrated in Figure 2.

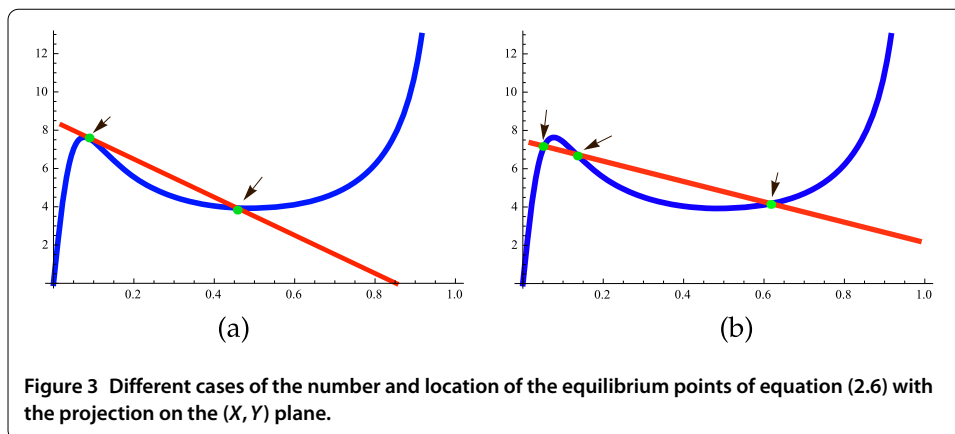
Next, consider the location and stability of the equilibrium points of equation (2.6), the equilibrium points are the intersecting nodes of the slow manifold and the curved surface,

$$\{(Z, Y, V, U) \mid Y = Y_{\max}(1 - \varrho X)\}.$$

The number and location of the equilibrium points are dependent on the parameters of the system; there may be one, two or three equilibrium points, as shown in Figure 1 and Figure 3 with the projection on the (X, Y) plane.

To decide on the stability of those equilibrium points, consider the characteristic equation

$$D(\lambda) = \lambda^4 + b\lambda^3 + c\lambda^2 + d\lambda + e = 0, \quad (3.4)$$



where

$$b = \varepsilon(2a - \varrho X_0),$$

$$c = \varepsilon(a^2 + \varrho X_0 - \varrho X_0^2) - \varepsilon^2 \cdot 2a\varrho X_0,$$

$$d = \varepsilon^2 \left[a\varrho X_0(2 - 2X_0 - a) + \frac{a^2 Y_0}{Y_{\max}} \right],$$

$$e = \varepsilon^2 a^2 \varrho X_0(1 - X_0).$$

When $\varepsilon = 0$, $D(\lambda) = 0$ has four characteristic roots

$$\lambda_0^i = 0, \quad i = 1, 2, 3, 4.$$

When $0 < \varepsilon \ll 1$, the three characteristic roots of $D(\lambda) = 0$ can be described as

$$\lambda_\varepsilon^1 = \varepsilon \kappa_1, \quad \lambda_\varepsilon^2 = \varepsilon \kappa_2, \quad \lambda_\varepsilon^3 = \varepsilon \kappa_3, \quad \lambda_\varepsilon^4 = \varepsilon \kappa_4,$$

where $\kappa_i = O(1)$ ($i = 1, 2, 3, 4$) are constant. The equilibrium point (Z_0, Y_0, V_0, U_0) is stable if and only if all the four characteristic roots λ_ε^i ($i = 1, 2, 3, 4$) are with a negative real part. Since e and c are always positive, the sign of λ_ε^i ($i = 1, 2, 3, 4$) is one of $(-, -, -, -)$, $(-, -, +, +)$, and $(+, +, +, +)$.

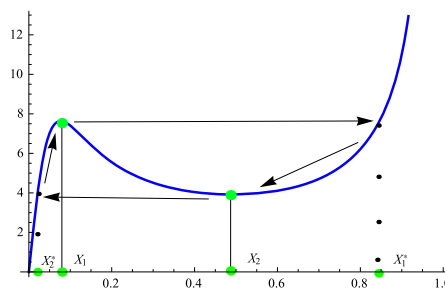
When $\varrho < \frac{2a}{X_0}$ and $\varrho X_0(2 - 2X_0 - a) + \frac{aY_0}{Y_{\max}} > 0$, one has $-b < 0$ and $-d < 0$, which leads to $\lambda_\varepsilon^i < 0$ ($i = 1, 2, 3, 4$) due to $\lambda_\varepsilon^1 + \lambda_\varepsilon^2 + \lambda_\varepsilon^3 + \lambda_\varepsilon^4 = -b < 0$ and $\lambda_\varepsilon^1 \lambda_\varepsilon^2 (\lambda_\varepsilon^3 + \lambda_\varepsilon^4) + \lambda_\varepsilon^3 \lambda_\varepsilon^4 (\lambda_\varepsilon^1 + \lambda_\varepsilon^2) = -d < 0$.

When $\varrho > \frac{2a}{X_0}$ or $\varrho X_0(2 - 2X_0 - a) + \frac{aY_0}{Y_{\max}} < 0$, one has $-b > 0$ or $-d > 0$, which leads to the sign of λ_ε^i ($i = 1, 2, 3, 4$) being either $(-, -, +, +)$ or $(+, +, +, +)$.

Thus, when the equilibrium point $(Z_0, Y_0, V_0, U_0) \in M_2$ and $\varrho > \frac{2a}{X_0}$ or $\varrho X_0(2 - 2X_0 - a) + \frac{aY_0}{Y_{\max}} < 0$, then the equilibrium point located in M_2 is unstable. When the equilibrium point $(Z_0, Y_0, V_0, U_0) \in M_1 \cup M_3$, $\varrho < \frac{2a}{X_0}$, and $\varrho X_0(2 - 2X_0 - a) + \frac{aY_0}{Y_{\max}} > 0$, then the equilibrium point located in $M_1 \cup M_3$ is stable.

Once the structure of the slow manifold M and the position and stability of the equilibria of equation (2.6) are obtained, the dynamical behaviors of equation (2.6) can be analyzed through the geometric singular perturbation theory.

Figure 4 The relaxation oscillation of equation (2.6) with the projection on the (X, Y) plane.



Conditions $\varrho < \frac{1}{X_2}$ and $-Y_{\max}\varrho > \frac{Y_2 - Y_1}{X_2 - X_1}$ guarantee that there is an equilibrium point in the slow manifold M_1 and M_3 , respectively, as shown in Figure 3(b). When $\frac{1}{X_2} < \varrho < \frac{1}{X_1}$ and $-Y_{\max}\varrho < -\frac{Y_1}{X_2 - X_1}$, there are no equilibrium points in the slow manifold $M_1 \cup M_3$, as shown in Figure 1. According to the geometric singular perturbation theory, the solution trajectory will be attracted by the stable manifold and repelled by the unstable manifold.

Remark 2 The original model (1.1) in [1] is a 2D system. The Jacobian J of the vector field defining the original system is given by second-order matrices. The authors used $\text{tr}(J)$ and $\det(J)$ to judge on the positive and negative of eigenvalues. However, the corresponding characteristic equation of our model is a quartic equation. Thus, the positive and negative judgment of eigenvalues is more complicated. Through the analysis of the characteristic equation, the positive and negative of characteristic roots were obtained.

When the solution trajectory is attracted by the stable slow manifold M_1 , it will stick to the stable manifold and move slowly from down to up, due to

$$\frac{dY}{d\tau} = Yf\left(\frac{Z}{Y}, V; \varrho, Y_{\max}\right) > 0$$

with $(Z, Y, V, U) \in M_1$. When the solution trajectory crosses the saddle-node bifurcation point B_1 , it will be repelled by the unstable slow manifold M_2 , and be attracted by the stable slow manifold M_3 quickly, then the solution trajectory will stick to M_3 and move slowly from up to down due to $\frac{dY}{d\tau} < 0$ with $(Z, Y, V, U) \in M_3$. When the solution trajectory crosses the saddle-node bifurcation point B_2 , it will be again attracted by M_1 quickly. Thus, the slow movement process alternates with the rapid movement process in the predator-prey system, and the predator-prey system undergoes relaxation oscillation, as shown in Figure 4.

Remark 3 Reference [1] used the attraction domain of the upper and lower stable branch of the quasi-steady state (16) to judge on the clockwise direction of the relaxation oscillation. In this paper, we use the sign of $\frac{dY}{d\tau}$ to judge on the clockwise direction of the relaxation oscillation. This method is simpler and clearer in comparison.

The relaxation oscillation of (1.2) is described approximately as

$$\begin{cases} Y = \frac{X}{(X^2 + \alpha^2)(1-X)}, & X \in (X_2^*, X_1], \\ Z = Y_1 X_1, & X \in (X_1, X_1^*], \\ Y = \frac{X}{(X^2 + \alpha^2)(1-X)}, & X \in [X_2, X_1^*), \\ Z = Y_2 X_2, & X \in [X_2^*, X_2), \end{cases} \quad (3.5)$$

where $\frac{X_i^*}{((X_i^*)^2 + \alpha^2)(1-X_i^*)} = Y_i^*$.

Since $0 < \varepsilon \ll 1$, the quick movement process of fast manifolds is instantaneous, thus, the period of the relaxation oscillation is governed by the slow movement process. Hence, from (3.2) the asymptotic expression for the period T of the relaxation oscillations to the lowest order in the perturbation parameter ε is [22–24]

$$\begin{aligned} T &= \int_{M_1} d\tau + \int_{M_3} d\tau + O(\varepsilon) \\ &\approx \int_{M_1} \frac{dY}{Yf(X, V; \varrho, Y_{\max})} + \int_{M_3} \frac{dY}{Yf(X, V; \varrho, Y_{\max})} \\ &= \int_{X_2^*}^{X_1} \frac{\Psi'(X) dX}{\Psi(X)f(X, \Psi(X); \varrho, Y_{\max})} + \int_{X_2}^{X_1^*} \frac{\Psi'(X) dX}{\Psi(X)f(X, \Psi(X); \varrho, Y_{\max})} \\ &= Y_{\max} \left(\int_{X_2^*}^{X_1} \frac{\mathbb{P}_3(X) dX}{X \mathbb{P}_4(X)} + \int_{X_1^*}^{X_2} \frac{\mathbb{P}_3(X) dX}{X \mathbb{P}_4(X)} \right), \end{aligned} \quad (3.6)$$

where $O(\varepsilon)$ is the so-called junction time governed by the fast movement process, and $\mathbb{P}_4(X) = Y_{\max} \varrho X^4 - Y_{\max} (1 + \varrho) X^3 + Y_{\max} (1 + \alpha^2 \varrho) X^2 - (1 + \alpha^2 Y_{\max} + \alpha^2 \varrho Y_{\max}) X + \alpha^2 Y_{\max}$.

In summary, the main results of this paper can be stated as follows.

Proposition *If one of the following two conditions holds:*

- (H₁) $\max\{\frac{1}{X_2}, \frac{2a}{X_2}, \frac{2a}{X_1}\} < \varrho < \frac{1}{X_1}, -Y_{\max} \varrho < -\frac{Y_1}{X_2 - X_1};$
 (H₂) $\frac{1}{X_2} < \varrho < \frac{1}{X_1}, -Y_{\max} \varrho < -\frac{Y_1}{X_2 - X_1},$ and $\varrho X_i (2 - 2X_i - a) + \frac{aY_i}{Y_{\max}} < 0$ ($i = 1, 2$),

then the predator-prey system undergoes relaxation oscillation, and the analytical expressions of the relaxation oscillation and its period are described approximatively as equations (3.5) and (3.6), respectively.

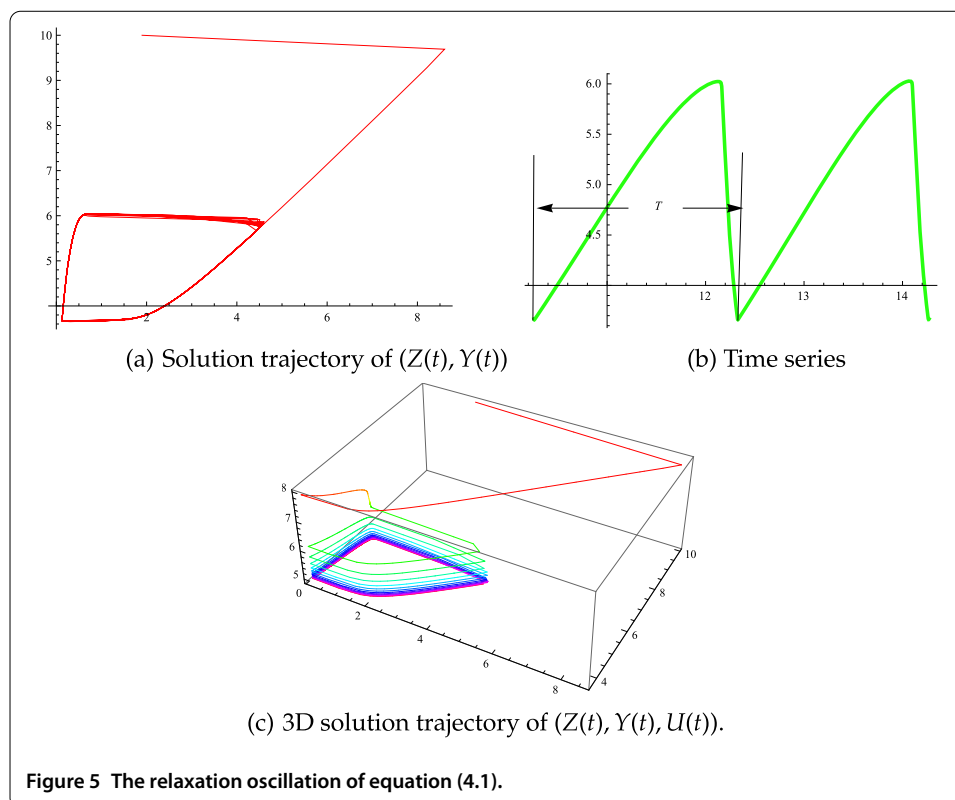
Remark 4 Conditions (H₁) and (H₂) are incompatible.

4 Numerical example

To demonstrate the validity of the analytical results obtained in the previous sections, two specific examples are studied in this section.

Example 1 Let $\varepsilon = 0.001$, $\alpha^2 = 0.0085$, $Y_{\max} = 16$, $\varrho = 5.5$, $a = 0.2$, equation (2.6) reads

$$\begin{cases} \frac{dZ}{dt} = Y[X(1-X) - \frac{1}{Y} \cdot \frac{X^2}{0.0085+X^2}], \\ \frac{dY}{dt} = \varepsilon Y(1 - \frac{V}{16} - 5.5X), \\ \frac{dV}{dt} = 0.2\varepsilon(U - V), \\ \frac{dU}{dt} = 0.2\varepsilon(Y - U), \end{cases} \quad (4.1)$$



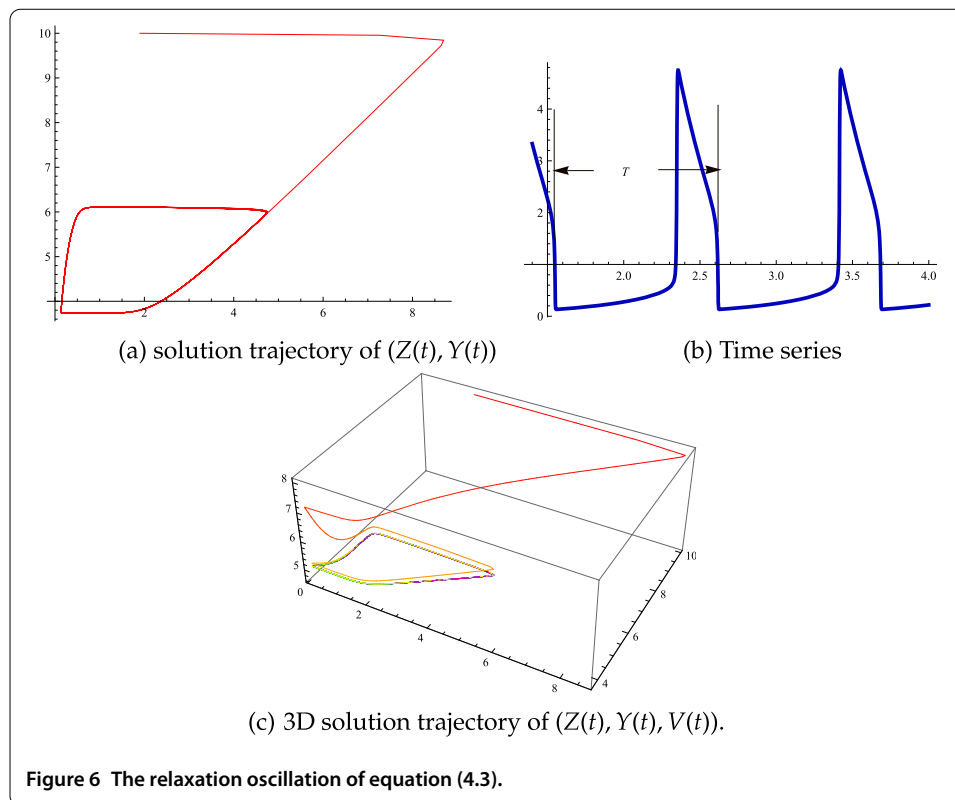
where $X = \frac{Z}{Y}$. By calculating on the platform of *Mathematica*, we have $X_1 = 0.103536$, $X_2 = 0.481682$, $Y_1 = 6.00913$, $Y_2 = 3.86382$, $X_1^* = 0.792927$, $X_2^* = 0.0366351$, $\frac{1}{X_2} = 2.07606$, $\frac{1}{X_1} = 9.65845$. It is easy to see that $\max\{\frac{1}{X_2}, \frac{2a}{X_2}, \frac{2a}{X_1}\} < \varrho = 5.5 < \frac{1}{X_1}$, $-Y_{\max}\varrho = -88 < -\frac{Y_1}{X_2 - X_1} = -15.891$. The system undergoes relaxation oscillation, this result is confirmed by the numerical result in Figure 5. From equation (3.5), the approximate expression of the relaxation oscillation is

$$\begin{cases} Y = \frac{X}{(X^2 + \alpha^2)(1-X)}, & X \in (0.0366351, 0.103536], \\ Z = 0.622161, & X \in (0.103536, 0.792927], \\ Y = \frac{X}{(X^2 + \alpha^2)(1-X)}, & X \in [0.481682, 0.792927], \\ Z = 1.86113, & X \in (0.0366351, 0.489569). \end{cases} \quad (4.2)$$

From equation (3.6), one obtains the approximate period of the relaxation oscillation $T_{\text{appr}} = 1.4124$, which agrees with the numerical result $T = 1.76242$.

Example 2 Let $\varepsilon = 0.001$, $\alpha^2 = 0.0085$, $Y_{\max} = 32$, $\varrho = 4$, $a = 3.7$, equation (2.6) reads

$$\begin{cases} \frac{dZ}{dt} = Y[X(1-X) - \frac{1}{Y} \cdot \frac{X^2}{0.0085 + X^2}], \\ \frac{dY}{dt} = \varepsilon Y(1 - \frac{V}{32} - 4X), \\ \frac{dV}{dt} = 3.7\varepsilon(U - V), \\ \frac{dU}{dt} = 3.7\varepsilon(Y - U), \end{cases} \quad (4.3)$$



where $X = \frac{Z}{Y}$. Since $\frac{1}{X_2} < \varrho = 4 < \frac{1}{X_1}$, $-Y_{\max}\varrho = -128 < -\frac{Y_1}{X_2 - X_1} = -15.891$, $\varrho X_1(2 - 2X_1 - a) + \frac{aY_1}{Y_{\max}} = -0.0949968 < 0$, and $\varrho X_2(2 - 2X_2 - a) + \frac{aY_2}{Y_{\max}} = -4.68482 < 0$, the system undergoes relaxation oscillation. This result is confirmed by the numerical result in Figure 6. From equation (3.6), one obtains the approximate period of the relaxation oscillation $T_{\text{appr}} = 0.94409$, which agrees with the numerical result $T = 1.05677$.

Remark 5 Though the two phase planes look very similar for the two cases, they represent two different cases which satisfy the incompatible conditions (H_1) and (H_2) .

5 Summary

In this paper the geometric singular perturbation theory is employed to illuminate the transition of the solution trajectory. The existence of the relaxation oscillation is also proved. Its validity is illustrated by two examples. The whole study is complemented with direct numerical simulations of the dimensionless spruce-budworm model (2.6).

Remark 6 By using the qualitative result (see the proposition), the existence of the relaxation oscillation of this kind of predator-prey system with distributed delay can be determined quickly. The figures of the solution which is obtained by mathematical software can be explained as the periodical change of ecological population, such as the period of pests outbreaks. After understanding the periodic system, we can control the pests outbreaks possibly by adjusting the model's parameters.

Remark 7 The studies indicate that this kind of predator-prey system with distributed delay can exhibit relaxation oscillation, which shows that the Hopfield predator-prey system has the potential to reproduce the complex dynamics of a real predator-prey system.

Competing interests

The authors declare that no conflict of competing interests exists.

Authors' contributions

NW carried out the main theorem and wrote this article. NW and MH read and approved the final manuscript.

Author details

¹Department of Applied Mathematics, Shanghai Institute of Technology, Shanghai, 201418, China. ²Department of Mathematics, Shanghai Normal University, Shanghai, 200241, China.

Acknowledgements

The authors are grateful to the editor and two referees for a number of helpful suggestions, which have greatly improved our original manuscript. This research is supported by National Science Foundation of China (No: 11401385).

Received: 3 August 2015 Accepted: 7 March 2016 Published online: 14 March 2016

References

1. Rasmussen, A, Wyller, J, Vik, JO: Relaxation oscillations in spruce-budworm interactions. *Nonlinear Anal., Real World Appl.* **12**, 304-319 (2011)
2. Ludwig, D, Jones, D, Holling, CS: Qualitative analysis of insect outbreak systems: the spruce budworm and forest. *J. Anim. Ecol.* **47**, 315-332 (1978)
3. Holling, CS: Some characteristics of simple types of predation and parasitism. *Can. Entomol.* **91**(7), 385-398 (1959)
4. Liu, WS, Xiao, DM, Yi, YF: Relaxation oscillations in a class of predator-prey systems. *J. Differ. Equ.* **188**, 306-331 (2003)
5. Muratori, S, Rinaldi, S: Remarks on competitive coexistence. *SIAM J. Appl. Math.* **49**, 1462-1472 (1989)
6. Rizaner, FB, Rogovchenko, SP: Dynamics of a single species under periodic habitat fluctuations and Allee effect. *Nonlinear Anal., Real World Appl.* **13**, 141-157 (2012)
7. Freedman, HI, Wolkowicz, GSK: Predator-prey systems with group defence: the paradox of enrichment revisited. *Bull. Math. Biol.* **48**(516), 493-508 (1986)
8. Yu, W, Cao, J: Stability and Hopf bifurcation analysis on four-neuron BAM neural network with time delays. *Phys. Lett.* **351**, 64-78 (2006)
9. Sun, C, Lin, Y, Han, M: Stability and Hopf bifurcation for an epidemic disease model with delay. *Chaos Solitons Fractals* **30**, 204-216 (2006)
10. Chen, Y, Yu, J, Sun, C: Stability and Hopf bifurcation analysis in a three-level food chain system with delay. *Chaos Solitons Fractals* **31**, 683-694 (2007)
11. Zheng, YG, Bao, LJ: Slow-fast dynamics of tri-neuron Hopfield neural network with two timescales. *Commun. Nonlinear Sci. Numer. Simul.* **19**, 1591-1599 (2014)
12. Farkas, M: *Periodic Motions*. Springer, New York (1994)
13. Britton, N: Spatial structures and periodic travelling waves in an integro differential reaction-diffusion population model. *SIAM J. Appl. Math.* **50**, 1663-1688 (1990)
14. Gourley, S, Britton, N: A predator prey reaction diffusion system with nonlocal effects. *J. Math. Biol.* **34**, 297-333 (1996)
15. Fargue, M: Réducibilité des systèmes héréditaires à des systèmes dynamiques. *C. R. Acad. Sci. Paris Sér. A-B* **227**, 471-473 (1973)
16. Ferreira, JD, Salazar, CA, Tabares, PC: Weak Allee effect in a predator-prey model involving memory with a hump. *Nonlinear Anal., Real World Appl.* **14**, 536-548 (2013)
17. Ma, ZP, Huo, HF, Liu, CY: Stability and Hopf bifurcation analysis on a predator-prey model with discrete and distributed delays. *Nonlinear Anal., Real World Appl.* **10**, 1160-1172 (2009)
18. Jones, C: *Geometric Singular Perturbation Theory in Dynamical Systems*. Springer, Berlin (1994)
19. Tikhonov, A: Systems of differential equations containing a small parameter multiplying the derivative. *Mat. Sb.* **31**, 575-586 (1952)
20. Fenichel, N: Asymptotic stability with rate conditions. *Indiana Univ. Math. J.* **23**, 1109-1137 (1974)
21. Fenichel, N: Geometric singular perturbation theory for ordinary differential equations. *J. Differ. Equ.* **31**, 53-98 (1979)
22. Mishchenko, EF, Rozov, NK: *Differential Equations with Small Parameters and Relaxation Oscillations*. Plenum, New York (1980)
23. Rozov, NK: Asymptotic computation of solutions of systems of second-order differential equations close to discontinuous solutions. *Sov. Math. Dokl.* **3**(4), 932-934 (1962)
24. Zharov, MI, Mishchenko, EF, Rozov, NK: On some special functions and constants arising in the theory of relaxation oscillations. *Sov. Math. Dokl.* **24**(3), 672-675 (1981)